Charge reversal of sulfate latex particles in the presence of lanthanum ion

Takuya Sugimoto [a,b], Manami Nishiya [b], and Motoyoshi Kobayashi [c]*

[a] Graduate School of Agricultural and Life Sciences, The University of Tokyo, 1-1-1 Yayoi, Bunkyou-ku, Tokyo 113-8657, Japan

[b] Graduate School of Life and Environmental Sciences, University of Tsukuba, 1-1-1 Tennoudai, Tsukuba, Ibaraki 305-8572, Japan

[c] Faculty of Life and Environmental Sciences, University of Tsukuba, 1-1-1 Tennoudai, Tsukuba, Ibaraki 305-8572, Japan

*Corresponding author

E-mail address: kobayashi.moto.fp@u.tsukuba.ac.jp

Abstract

Effects of multivalent cations and its hydrolyzed forms on the charge reversal are investigated by measuring electrophoretic mobilities of three different sulfate latex particles bearing pH-independent surface charge densities as a function of $LaCl_3$ concentration and pH. The obtained experimental results are analyzed by using a simple adsorption model including an ion-ion correlation model, intrinsic energy of adsorption for hydrolyzed La ions, and the speciation calculation of La. From the experimental electrophoretic mobilities at pH=4 without hydrolyzed La ions, we observed that the $LaCl_3$ concentrations at charge reversal increased with decreasing the magnitude of the latex charge density. This experimental trend can be qualitatively captured by the ionic correlation model used here. While the sulfate latex particles bear pH-independent surface charge and the $LaCl_3$ concentration was lower than the concentration where the charge reversal took place at pH 4, the increase in pH significantly gave rise to the charge reversal at pH above 7.8 where the hydrolyzed La ions begin to form. Therefore, this charge reversal at higher pH can be assigned to the stronger adsorption of hydrolyzed La ions. In addition, we demonstrate that the simple model can capture such experimental trends of charge reversal by introducing surmised values of its intrinsic energy of adsorption. Therefore, our results confirm that the ion correlation can be a prevailing mechanism on the charge reversal at low pH, while the stronger adsorption of hydrolyzed La ions predominates to induce the reversal with increasing pH.

Key words: Electrophoresis; Charge inversion; Lanthanum ion; Hydrolyzed ion

1. Introduction

The stability of colloidal dispersion against aggregation is important in industrial and environmental processes such as painting materials, paper production, waste water treatment, and colloid-facilitated transport[1]–[3]. The aggregation and dispersion of charged colloidal particles can be generally controlled by the balance of the van der Waals attraction and electrostatic force, according to so-called the DLVO theory after its founders of the Derjaguin, Landau, Verwey, and Overbeek[4], [5]. Especially, the electrostatic force relies on the charging state of colloids and the concentration and types of ions. Therefore, we need to evaluate the surface charge of colloidal particles at different ionic concentrations to predict their colloid stability against aggregation.

The surface charges of particles are strongly modulated with the co-existence of counter ionic species such as polyelectrolytes[6]–[9], surfactants[10]–[13], multivalent ions[14]–[19], proteins[20], and specifically-adsorbing ions[21]–[24], which have stronger tendency to adsorb onto the surface. Their adsorption can lead to the charge reversal/overcharging causing the change in sign of the net surface charges due to the excess adsorption of oppositely-charged species[25]. Many researchers have been trying to clarify the prevailing mechanism of charge reversal with the approaches of Monte-Carlo simulation, molecular dynamics and strong coupling theory including ion correlation[26]–[30], ionic specificity[31], and hydrophobic interaction[32]. Remarkably, their theory on ionic correlation has explained reasonably well the charge reversal for the colloidal system with multivalent counter ions such as La^{3+} ions[29] and ferricyanide ions[33]. However, such multivalent ions can be hydrolyzed with increasing pH and their ionic valence is decreased due to the binding of hydroxyl ions[34]. Although such hydrolyzed ions have decreased the ionic valence, they can strongly adsorb onto the charged surface and induce measurable charge reversal[14], [35], [36]. This phenomenon cannot be explained by the ion correlation mechanism. The significance of hydrolysis compared to the ion correlation was emphasized in the previous study[14], [35]. Neverthelss, the effect of surface charge density on charge reversal with hydrolysis is overlooked. It still remains ambiguous due to the lack of systematic experimental data and comprehensive theoretical modeling for the particles bearing pH-independent surface charged groups with different surface charge densities.

In this study, to gain further insight into the effect of multivalent cations and their hydrolyzed forms on the charge reversal, we measured the electrophoretic mobilities of three different polystyrene sulfate latex particles as a function of $LaCl_3$ concentration and pH. The sulfate latex particles have pH-independent surface charges owing to sulfate groups on their surface, which are fully deprotonated in the range of usual pH. This feature of sulfate latex particles with three different charge densities allows us to examine the effect of charge density and hydrolyzed ions on the charge reversal without changing their charged amount with pH. The obtained experimental results are analyzed with a simple model[33] including both an ion-ion correlation model[30] and

its intrinsic energy of adsorption[22], [37] for hydrolyzed La ions. To our knowledge, it should be noted that such experimental verification of the model including both ion-ion correlation and specific adsorption for hydrolyzed ions has been examined for the first time.

2. Materials and Methods

2.1 Materials

Three types of polystyrene sulfate latex (SL) particles (Molecular Probes, Inc.) were employed as model colloidal particles. Sulfate latex particles have pH-independent negative charges due to the deprotonated sulfate groups on the particle surface. These suspensions were dialyzed using Visking tube against de-ionized water. The manufacturer reports their density, diameter $2a$ and surface charge density σ_0 obtained by conductometric titration as tabulated in Table 1. However, we have measured the electrophoretic mobilities of the same particles as a function of KCl concentration and reported that the electrokinetic surface charge density of the particles can be different from the values provided by the manufacturer to achieve the reasonable agreement between experiments and theory as shown in Table 1 [21]. Thus, the reported values of electrokinetic surface charge density by the previous work [21] are used as the surface charge densities for the following theoretical analysis in this study. $LaCl_3 \cdot 7H_2O$ (JIS special grade, Wako Pure Chemical Industries) was used to prepare the electrolyte solutions. The pH was adjusted by the addition of HCl (JIS special grade, Wako Pure Chemical Industries) and KOH solutions. Carbonate free KOH solution was prepared by following the method described in the literature[38]. Before the sample preparation, all solutions were filtered with a 0.20 μm pore filter (DISMIC 25HP ADVANTEC). All solutions and suspensions were prepared from deionized degassed water (Elix, MILLIPORE) and degassed before use.

2.2 Experimental methods

Electrophoretic mobility (EPM) was measured by electrophoretic light scattering technique with Zetasizer NANO-ZS (Malvern). Two series of measurements were carried out. One was measurement as a function of $LaCl_3$ concentration, and the other was varying solution pH. For the first one, $LaCl_3$ concentration was varied in the range from 0.001 mM to 100 mM at fixed pH 4. For the second measurements, the pH was adjusted in the range from 3 to 11 with HCl and KOH solutions at 0.01 mM, 0.1 mM, 1 mM and 10 mM in ionic strength. The particle concentration was set to 5 mg/L in all experiments. The samples were prepared by mixing the required volumes of one of three sulfate latex suspensions, $LaCl_3$ solution, pH adjuster, and

123 degassed water. The pH was measured by a combination electrode (ELP-035, TOA-DKK). All
124 experiments were carried out at 20 ℃.
125
126
127
128 **3. Theoretical Modeling**
129
130 *3.1 Chemical equilibria and hydrolysis for lanthanum species*
131 To model the effect of hydrolysis of La^{3+} ion on the particle charging behavior, we consider
132 the chemical equilibria in aqueous $LaCl_3$ solution. In the aqueous solution, one considers the
133 dissociation of $LaCl_3$ and water, and the hydrolysis of La^{3+} ions, as given by the following
134 equilibria [34]

$$LaCl_3 \rightleftharpoons La^{3+} + 3Cl^- \quad (1),$$

$$La^{3+} + H_2O \rightleftharpoons LaOH^{2+} + H^+ \quad : \widetilde{K}_1 \quad (2),$$

$$La^{3+} + 2H_2O \rightleftharpoons La(OH)_2{}^+ + 2H^+ \quad : \widetilde{K}_2 \quad (3),$$

$$La^{3+} + 3H_2O \rightleftharpoons La(OH)_3 + 3H^+ \quad : \widetilde{K}_3 \quad (4),$$

$$H_2O \rightleftharpoons H^+ + OH^- \quad : \widetilde{K}_w \quad (5),$$

135 where $\widetilde{K}_1$, $\widetilde{K}_2$, $\widetilde{K}_3$ are hydrolysis constants, and $\widetilde{K}_w$ is the ionic product of water. From the law of
136 mass action, the hydrolysis constants can be related to the concentration of each species as follows

$$\widetilde{K}_1 = 10^{\log_{10}\widetilde{K}_1} = \frac{[LaOH^{2+}][H^+]}{[La^{3+}]} \quad (6),$$

$$\widetilde{K}_2 = 10^{\log_{10}\widetilde{K}_2} = \frac{[La(OH)_2{}^+][H^+]^2}{[La^{3+}]} \quad (7),$$

$$\widetilde{K}_3 = 10^{\log_{10}\widetilde{K}_3} = \frac{[La(OH)_3][H^+]^3}{[La^{3+}]} \quad (8),$$

$$\widetilde{K}_w = 10^{\log_{10}\widetilde{K}_w} = [H^+][OH^-] \quad (9),$$

137 where we use the values of $\log_{10}\widetilde{K}_1 = -8.6$, $\log_{10}\widetilde{K}_2 = -17.9$, $\log_{10}\widetilde{K}_3 = -27.3$ from the
138 literature [39], and $\log_{10}\widetilde{K}_w = -13.997$.
139 For a given total concentration C_{tot} of lanthanum species in a solution, the mass
140 conservation law is expressed with the following equation

$$C_{tot} = [La^{3+}] + [LaOH^{2+}] + [La(OH)_2{}^+] + [La(OH)_3] \quad (10).$$

141 In addition, the electroneutrality condition is fulfilled in the solution given by

$$3[La^{3+}] + 2[LaOH^{2+}] + [La(OH)_2{}^{+}] + [H^+] + [K^+] - [OH^-] - [Cl^-] = 0 \quad (11)$$

where $[H^+] = 10^{-pH_0 - dpH}$ is the proton concentration after hydrolysis reaction, pH_0 is the initial pH, and dpH is the pH variation due to the hydrolysis of La^{3+} ions. Here, we assume that Cl^- and K^+ ions also come from the addition of HCl below pH=7 and KOH above pH=7 to adjust solution pH, respectively. The bulk concentration of La^{3+} ions and its hydrolysed forms were obtained by solving the set of Eqs. (6–11) numerically.

3.2 Charging model

The La^{3+} ions interact with each other near the charged surface due to its finite size and electric repulsion. Such effects are called ion correlation effects and cannot be described by the classical Poisson-Boltzmann equation, which treats ions as point charges and neglects inter-ion interactions. To include ion correlation effects, many researchers have proposed various approaches[30], [40]–[42]. In this study, we employ the formulation proposed by Shklovski [30], whose expression is based on the theoretical assumption that multivalent counter-ions should form a strongly correlated ionic solution in the Stern layer on highly-charged surfaces. Such effects on surface adsorption of La^{3+} ions can be included into the Stern layer model via the additional energy per ion ϕ_{ic} due to spatial interactions between La^{3+} ions in the Stern layer by using the following equation[10], [33]:

$$\Gamma_s = 2r_s C_{La^{3+}} \exp\left(-\frac{3e\psi_d - \phi_{ic}}{k_B T}\right) \quad (12)$$

where Γ_s is the ionic density of La^{3+} ions in the Stern layer, r_s is the hydrated ionic radius of La^{3+} ion, $C_{La^{3+}}$ is the bulk concentration of La^{3+}, e is the elementary charge, ψ_d is the diffuse layer potential, k_B is the Boltzmann constant, and T is the absolute temperature. The additional energy ϕ_{ic} in Eq.(12) is given by

$$\phi_{ic} = k_B T\left(1.65\Gamma_{ic} - 2.61{\Gamma_{ic}}^{1/4} + 0.26\ln\Gamma_{ic} + 1.95\right) \quad (13)$$

with the interaction parameter Γ_{ic} of

$$\Gamma_{ic} = \frac{1}{4k_B T\varepsilon_r\varepsilon_0}\sqrt{\left|\frac{(ze)^3\sigma_0}{\pi}\right|} \quad (14),$$

where $\varepsilon_r\varepsilon_0$ is the dielectric constant of water, z is the ionic valence, namely, $z = 3$ for La^{3+} ion, and σ_0 is the surface charge density of bare surfaces. This formulation holds for $\Gamma_{ic} \gg 1$ [30], which is typically satisfied for $z \geq 3$. For this reason, we apply Eqs. (13) and (14) only for La^{3+} ion, not for its hydrolysed forms.

With Eqs. (12–14), we can express the Stern layer charge density σ_s without hydrolysis of La^{3+} ion as

$$\sigma_s = 3eN_A\Gamma_s \tag{15}$$

where N_A is the Avogadro number. This equation suggests that the ionic density of La^{3+} ions in the Stern layer is in charge of the development of the Stern layer charge density σ_s.

Above a certain pH where the hydrolyzed La ions are formed, one can generalize Eqs. (12) and (15) to include the contribution from the hydrolyzed La ions, namely,

$$\Gamma_i = 2r_{s_i}C_{i,b}\exp\left(-\frac{z_i e\psi_d - \phi_i}{k_B T}\right) \tag{16}$$

$$\sigma_s = \sum_{i=1}^{N} z_i e N_A \Gamma_i \tag{17}$$

where Γ_i is the ionic density of each species in the Stern layer, r_{s_i} is the hydrated ionic radius, $C_{i,b}$ is the bulk concentration, z_i is the ionic valence, and ϕ_i is the non-electrostatic or intrinsic adsorption energy of ions. Here, the index i denotes each ionic species. For the adsorption energy of La^{3+} ions, we have employed Eq.(13), namely, $\phi_{La^{3+}} = \phi_{ic}$, and the ones for its hydrolyzed forms of $LaOH^{2+}$ and $La(OH)_2^{+}$ are treated as fitting parameters. We have chosen the values for the hydrolyzed ions by the calculations with different sets of the intrinsic energy of adsorption to reasonably capture the experimental trends. The detailed calculations are summarized as the supplementary material. In Eq.(16), we have estimated the value of the hydrated ionic radius r_{s_i} for La^{3+} ions as its hydrodynamic radius obtained from the relationship between the ionic mobility under an electrical field and the limiting equivalent conductance[43], [44] as

$$r_{s_i} = \frac{|z|e^2 N_A}{6\pi\eta_s \Lambda^{\circ}_{La^{3+}}} \tag{18}$$

where $|z|$ is the absolute value of the ionic valence which is $|z| = 3$, η_s is the viscosity of the solution, and $\Lambda^{\circ}_{La^{3+}}$ is the limiting equivalent conductance of La^{3+} ions. The diameter of the hydrated La^{3+} ion is $2r_{s_i} = 0.784$ nm, and also we approximately used this value as the values of hydrated ionic diameter for $LaOH^{2+}$ and $La(OH)_2^{+}$ ions because the values of limiting equivalent conductance for the hydrolyzed ions are unavailable to the best of our knowledge.We also have discussed that the effects of the values of hydrated radii for the hydrolyzed ions on the EPMs are not so significant. The detailed disucussions are summarized in the supplementary material.

The relationship between the diffuse layer charge density σ_d and the diffuse layer potential ψ_d for our system is given by integrating the Poisson-Boltzmann equation for general electrolyte

196 solutions once as follows[45]:

$$\sigma_d = -\frac{\varepsilon_r \varepsilon_0 \kappa k_B T}{e} \mathrm{sgn}(\psi_d) \left[\frac{2 \sum_{i=1}^{N} C_{i,b} \left(\exp\left(-\frac{z_i \psi_d}{k_B T} \right) - 1 \right)}{\sum_{i=1}^{N} z_i^2 C_{i,b}} \right]^{\frac{1}{2}} \quad (19)$$

197 with the Debye parameter κ as

$$\kappa = \left(\frac{N_A e^2 \sum_{i=1}^{N} z_i^2 C_{i,b}}{\varepsilon_r \varepsilon_0 k_B T} \right)^{\frac{1}{2}} \quad (20)$$

198 where $\mathrm{sgn}(\psi_d) = +1$ if $\psi_d > 0$, otherwise, $\mathrm{sgn}(\psi_d) = -1$ if $\psi_d < 0$.

199 From the electroneutrality condition, the sum of surface σ_0, the Stern layer σ_s, and diffuse
200 layer charge densities σ_d must be zero, that is,

$$\sigma_0 + \sigma_s + \sigma_d = 0 \quad (21)$$

201 The set of Eqs. (12-20) is solved numerically to obtain the diffuse layer potential ψ_d for the
202 successive calculation of the zeta potential ζ. Particularly, we assume that no hydrolyzed forms
203 of La^{3+} ions are present in the analysis of electrophoretic measurements as a function of $LaCl_3$
204 concentration at pH 4 where no hydrolysis happens.

205 For the calculation of the electrophoretic mobility in the following section, the zeta potential
206 $\zeta = \psi(x_s)$ is calculated from ψ_d by integrating the following equation from the plane of diffuse
207 layer potential to the distance to the slipping plane x_s [45]

$$\frac{d\psi}{dx} = -\frac{\kappa k_B T}{e} \mathrm{sgn}(\psi(x)) \left[\frac{2 \sum_{i=1}^{N} C_{i,b} \left(\exp\left(-\frac{z_i \psi(x)}{k_B T} \right) - 1 \right)}{\sum_{i=1}^{N} z_i{}^2 C_{i,b}} \right]^{\frac{1}{2}} \quad (22),$$

208 where x_s is approximated to be equivalent to the diameter of La^{3+} ions as $2r_s = 0.784$ nm.
209
210
211 *3.2 Electrophoretic mobility (EPM)*
212 The electrophoretic mobilities (EPMs) are calculated from the zeta potential using the
213 Smoluchowski equation neglecting the relaxation effect of diffuse double layer. An electrokinetic
214 software, CellMobility, taking into account for the relaxation effect provided by the authors of
215 Refs. [46]–[48] is used to calculate EPMs in mixed electrolytes solution of $LaCl_3$ and HCl or
216 KOH. While the program can also calculate the dynamic electrophoretic mobilities in alternating
217 electric field with finite volume fraction of particles, the calculations reduce to the static
218 electrophoretic mobilities in electrostatic field with infinite dilute volume fraction such as
219 O'Brien-White model [49] when one chooses the frequency of the electric field less than 100 Hz
220 and the volume fraction less than 0.01. Therefore, we chose the values of 10 Hz for the frequency

and 0.001 for the volume fraction in our calculations. These conditions are satisfied throughout our experiments. The most significant advantage of the program is that it can include several ionic species in the model like O'Brien-White model[49]. This is essential to our analysis because the solution can contain not only $LaCl_3$, but also HCl, KOH, and the hydrolyzed forms of La^{3+} ions in higher pH as described by the above equilibria.

First, the Smoluchowski equation is given by

$$\mu_m = \frac{\varepsilon_r \varepsilon_0}{\eta_s} \zeta \tag{23}$$

where μ_m is the electrophoretic mobility.

Second, the CellMobility program requires the values of the limiting equivalent conductance of the *i*-th ionic species Λ_i°. In this study, the values of Λ_i° (10^{-4} S m^2/mol) used are 66.17 for K^+, 325.77 for H^+, 62.64 for La^{3+}, 68.68 for Cl^-, and 180.18 for OH^- which are taken from the literature[43], [44]. In addition, we use the same value of Λ_i° for La^+ as a first approximation to the values of Λ_i° for its hydrolyzed forms of $La(OH)^{2+}$ and $La(OH)_2^+$.

4. Results and Discussion

4.1 Electrophoretic mobility at pH 4 without La hydrolysis

We show the electrophoretic mobilities (EPMs) of the three different sulfate latex particles as a function of $LaCl_3$ concentration at pH 4 in Figures 1-3. Figure 1 is for the particles with the electrokinetic surface charge density $\sigma_0 = -11$ mC/m^2, Fig. 2 for ones with $\sigma_0 = -37$ mC/m^2, and Fig. 3 for ones with $\sigma_0 = -43$ mC/m^2, respectively. In these figures, the symbols are experimental values, the solid lines are the theoretical values calculated by the CellMobility program taking account of the relaxation effect, and the dashed lines are the theoretical values calculated by the Smoluchowski equation neglecting the relaxation effect. The thick lines are obtained with the model including the ion correlation effect using Eq.(13). The thin lines are calculated with no ion correlation assuming $\phi_{ic} = 0\ k_BT$. The values of the adsorption energy due to the ion correlation effect by Eq.(13) are $\phi_{ic} = 1.93$, 3.95, and 4.31 k_BT for $\sigma_0 = -11$, -37, and -43 mC/m^2, respectively. In addition, the calculated values in Figures 1-3 (a) are based on the assumption $\zeta = \psi_d$. For ones in Figures 1-3 (b), we assume $\zeta = \psi(x_s)$ with $x_s = 0.784$ nm.

The experimental electrophoretic mobilities of these particles increased with increasing $LaCl_3$ concentration and showed similar values below 0.2 mM irrespective of their surface charge density as shown in Figures 1-3. On the other hand, we observed the surface charge density

dependence of their EPMs in the concentration of 1 to 100 mM. That is, their absolute values decreased as the surface charge density increased. Particularly, the EPMs of the particles with $\sigma_0 = -37$ and -43 mC/m^2 showed positive values, namely, the charge reversal around 10 mM. This reversal is due to the charge overcompensation of La^{3+} ions[25], [33]. However, the EPMs decreased and became negative again with increasing $LaCl_3$ concentration. This decrease of EPMs followed with charge re-reversal could be attributed to the electrical screening in higher ionic strength and the screened electrical attraction between their surface and La^{3+} ions.

From the comparison between the experimental and theoretical values, such decreased behaviors of EPM in higher $LaCl_3$ concentration can be captured by introducing the slipping plane shown in Figures 1-3 (b), otherwise, the EPMs calculated with ion correlation effect progressively increase and are overestimated as depcited in Figures 1-3 (a). On the other hand, the calculations with relaxation effect (CellMobility) reasonably describe the experimental nonlinear dependence of EPM on $LaCl_3$ concentration. On the contrary, the Smoluchowski equation without relaxation effect shows disagreements with the epxeriment in low $LaCl_3$ concentration. Therefore, we employ the CellMobility with the slipping plane to analyze the experimental results in the following section.

Furthermore, one finds that the calculated values without ion correlation term ϕ_{ic} in Eq.(16) for the particle with $\sigma_0 = -11$ mC/m^2 do not show significant charge reversal, and the calculations agree well with the experimental ones as shown in Figure 1 (b). This result suggests that the ion correlation effect is not indicative for weakly-charged particles, which is consistent with the previous report based on experiments and a Monte-Carlo simulation[50]. Otherwise, the modeling needs to include the term ϕ_{ic} to the adsorption energy for the particles with $\sigma_0 = -37$ and -43 mC/m^2 so that it reproduces the charge reversal and achieves its qualitative agreements with the experimental results as shown in Figures 2 and 3 (b). Especially, the theoretical values for $\sigma_0 = -43$ mC/m^2 quantitatively capture its experimental charge reversed concentration, while ones for $\sigma_0 = -37$ mC/m^2 underestimate the reversed concentration. These results could be rationalized with the assumption of highly-charged surfaces for the use of Eq.(13), namely, $\Gamma_{ic} \gg 1$ defined in Eq.(14) [30]. This assumption seems to remain valid for the highest charged particles with $\Gamma_{ic} = 3.4$, while it is not valid for the lowest charged particles with $\Gamma_{ic} = 1.7$. According to above results, we decided to include the term ϕ_{ic} in Eq.(16) for $\sigma_0 = -37$ and -43 mC/m^2, while it is neglected for $\sigma_0 = -11$ mC/m^2 in the following section.

4.2 Electrophoretic mobility against pH with La hydrolysis

Prior to showing the results of pH dependence of EPMs, we show the calculated concentration

of La^{3+} ions and its hydrolyzed forms as a function of pH in Figure 4. This representative result is calculated for aqueous $LaCl_3$ solution with ionic strength of 10 mM. The blue line is for unhydrolyzed La^{3+} species. The red, green, and purple lines are for hydrolyzed La species such as $LaOH^{2+}$, $La(OH)_2^+$, and $La(OH)_3$, respectively. It should be noted that the $LaOH^{2+}$ ions start to form around pH 7 and $La(OH)_2^+$ around pH 8. The effect of formation of the hydrolyzed species on the EPMs is discussed in the following parts.

We plot the EPMs of the three different sulfate latex particles as a function of pH at different ionic strengths in Fig. 5 for the particles with the electrokinetic surface charge density $\sigma_0 = -11\ \mathrm{mC/m^2}$, Figure 6 for ones with $\sigma_0 = -37\ \mathrm{mC/m^2}$, and Figure 7 for ones with $\sigma_0 = -43\ \mathrm{mC/m^2}$, respectively. Green squares, red triangles, closed blue circles, and opened black circles are experimental values at ionic strengths *I* of 0.01, 0.1, 1, and 10 mM calculated from $LaCl_3$ concentration, respectively. The same colors, which correspond to the ionic strengths, are used for the theoretical curves calculated with the CellMobility program including the relaxation effect in Figures 5-7. The simple model Eq.(16) without the intrinsic adsorption energy of hydrolyzed La ions is used to calculate their EPMs in Figures 5-7 (a), while the adsorption energy of hydrolyzed La ions are included in Figures 5-7 (b).

At low pH, irrespective of ionic strength and their surface charge density, all particles did not show positive values of EPMs, namely, no charge reversal occurs as shown in Figures 5-7. The experimental EPMs in *I*=0.01 and 0.1 mM increased with pH below 6. This is due to the relaxation effect with decreasing added amounts of HCl which contribute to ionic strength[49], [51]. Such relaxation effects from added HCl is not so significant at *I*=1 and 10 mM because of less decrease in ionic strength. EPMs are constant up to pH 7. These behaviors can be excellently described by the calculated curves with the CellMobility program including relaxation effects.

In contrast to the result at low pH, the experimental EPMs at high pH and 1 and 10 mM were reversed to positive values in the range of $2 - 5 \times 10^{-8}\ \mathrm{m^2V^{-1}s^{-1}}$. The behavior indicates that significant charge reversal occurs above pH=7.6, where the $LaOH^{2+}$ species begins to form, and it is followed by $La(OH)_2^+$ above pH=8 and $La(OH)_3$ above pH=8.5 as noted in Figure 4. Since the charge reversed pH is consistent with the one at the hydrolysis starts, this charge reversal in high pH region can be attributed to the excess adsorption of the hydrolyzed La species onto the sulfate latex particles[14], [25]. This result suggests that the formation of the hydrolyzed La species and their adsorption are crucial on the charge reversal due to their strong affinity onto the particle surface even though only 6-7% of La species exist as $LaOH^{2+}$ ions at the charge reversed pH. In addition, it should be noted that the hydrolyzed La ions are essential to cause charge reversal even on the sulfate latex particles bearing pH-independent charges. This result suggests less importance of the complexation with pH-dependent charging groups such as SiOH and COOH[14]. Such charge reversal has been reported with sulfate latex particles not only in $LaCl_3$

solution, but also in $AlCl_3$ solution at higher pH where hydrolyzed $AlOH^{2+}$ ions are formed[35]. They also concluded that such reversal is attributed to the specific adsorption of hydrolyzed Al ions by comparing with speciation calculation of aluminum (III) as a function of pH[35]. On the other hand, we observed positive EPMs about 1×10^{-8} $m^2V^{-1}s^{-1}$ showing slight charge reversal at pH=7.8 in 0.1 mM followed by charge re-reversal in higher pH. This means that the amount of hydrolyzed La ions at 0.1 mM is not sufficient to cause significant reversal, and the EPM reversed again because of the reduced electrostatic attraction between the particle surface and hydrolyzed ions as a result of their decreased ionic valence and increased ionic strength by adding more KOH in higher pH. After this charge re-reversal, the EPMs at 0.1 mM decreased more with increasing pH, and the ones at 0.01 mM showed the same tendency without charge reversal. The decrease of EPMs in higher pH might be caused by diminished relaxation effects due to the increase of ionic strength with increasing pH, as an inverse case to the increased EPMs from pH=3 to 6 where ionic strength decreases with reducing the added amount of HCl.

In comparison with the calculated values, one finds that the simple adsorption model of Eq.(16) including the ion correlation term of Eq.(13) [30] without the intrinsic adsorption energy for the hydrolyzed ions, results in the negative values of EPMs with no charge reversal irrespective of pH and ionic strength as shown in Figures 5-7(a). However, once we introduce the values of 5 and 9.5 k_BT for the intrinsic adsorption energy of $LaOH^{2+}$ and $LaOH_2^+$ ions in Eq.(16), respectively, the calculated EPMs in 1 and 10 mM are positive at higher pH, namely, the charge reversal occurs around pH=8. This reversal trend qualitatively agrees with the experimental results as plotted in Figures 5-7(b). These results from our experiments using latex particles with pH-independent charge confirm that the introduction of the intrinsic adsorption energy of the hydrolyzed ions is unavoidable to model the charging behavior in systems containing hydrolyzable ions. Particularly, the calculated values for the sulfate latex particles with the charge density of $\sigma_0 = -11$ mC/m^2 describe well the experimental ones such as the maximum EPMs in 1 and 10 mM after charge reversal, the increase and subsequent decrease of EPMs in 0.1 mM with increasing pH, even without charge reversal as shown in Figure 5(b). However, Figures 6 and 7(b) show that the calculations for 0.1, 1 and 10 mM after charge reversal underestimate the experimental values more with increasing the magnitude of their charge density. This discrepancy could result from increasing ionic valence of the hydrolyzed La ions owing to dehydrolysis near the negatively charged particle surface where the proton concentration can be locally higher than the bulk, namely, lower pH. Such locally lower pH might induce shifts of chemical equilibria to reduce their amount of the hydrolyzed ions when they adsorb onto the surface. However, we do not include such process into our simple modeling, so we remain to address this issue in the future study.

To achieve the better agreement, we need to increase the magnitude of intrinsic adsorption

energy of the hydrolyzed ions with decreasing their ionic valence due to hydrolysis. This increase in their adsorption energy infers that the adsorption energy of the hydrolyzed ions cannot be explained by the ionic correlation model of Eq.(13) [30], which has its positive proportionality on valence, that is, $\phi_{ic} \propto \sqrt{z^3\sigma_0}$. Moreover, such increase in the intrinsic adsorption energy might be related to less hydrated state of the hydrolyzed ions because of their smaller valence and larger ionic radius expected from the binding with more hydroxyl ions. Such picture likely reduces the attractive interaction with water molecules.

5. Conclusion

Electrophoretic mobilities (EPM) of three different sulfate latex particles with pH-independent surface charge densities were measured as a function of $LaCl_3$ concentration and pH at several ionic strengths to clarify the effect of multivalent cations and its hydrolyzed forms on the charge reversal. As for the results of EPM as a function of $LaCl_3$ concentration at pH=4 where no hydrolysis occurs, we observed the charge reversal around 3 mM for the charge density of $\sigma_0 = -43\ \mathrm{mC/m^2}$, 10 mM for $-37\ \mathrm{mC/m^2}$, and no charge reversal for $-11\ \mathrm{mC/m^2}$. That is, the concentration at the reversal increased with decreasing the magnitude of their charge density. This experimental trend can be explained by the employed simple adsorption model with the ion-ion correlation model[30], notably, it showed the quantitative agreement on the reversed concentration with the experiments for the highest charge particles.

On the other hand, the EPM as a function of pH in ionic strengths of 1 and 10 mM showed the significant charge reversal around pH=7.6, where the hydrolyzed $LaOH^{2+}$ ions are formed according to the speciation calculation of La ions. The charge reveral was significant even though the corresponding $LaCl_3$ concentrations of 0.167 and 1.67 mM were less than the concentration where charge reversal occurs at pH=4 and the particle carried pH-independent surface charge as mentioned above. As a consequence, this charge reversal at higher pH is ascribed to the specific adsorption of the hydrolyzed La species. Furthermore, we have examined the effect of introducing their intrinsic adsorption energy onto the particle surface by using the presumable values, and showed that the model captures these experimental results. To the authors' knowledge, such comprehensive comparison between the experimental results and the simple model including both ion-ion correlation and the specific adsorption of the hydrolyzed ions has been performed for the first time. From the above results, therefore, we concluded that the ion-ion correlation can explain the charge reversal at low pH, while the excess adsorption of the hydrolyzed ions is essential to describe the reversal at higher pH. This implies that the aggregation of colloidal particles could be facilitated around the pH where hydrolyzed ions are formed in the co-existence of potentially

hydrolyzing ionic species in aqueous solution.

Acknowledgment

This work was supported by JSPS KAKENHI Grant Number 15H04563, 16H06382 and 18J00823. TS would like to thank to Prof. K. Higashitani and Prof. Y. Adachi for fruitful discussions.

Conflict of interest

The authors declare that they have no conflict of interest associated with this article.

Table 1 Properties of sulfate latex particles [21]

Property	Particle 1	Particle 2	Particle 3
Diameter $2a$ [μm]	0.25	0.47	1.2
Density [g/cm^3]	1.055	1.055	1.055
Surface charge density σ_0 [mC/m^2] *1	−6	−49	−96
Electrokinetic surface charge density σ_{ek} [mC/m^2] *2	−11	−37	−43

*1 Obtained from conductometric titration

*2 Obtained from analysis of electrophoretic mobility in KCl solution [21]

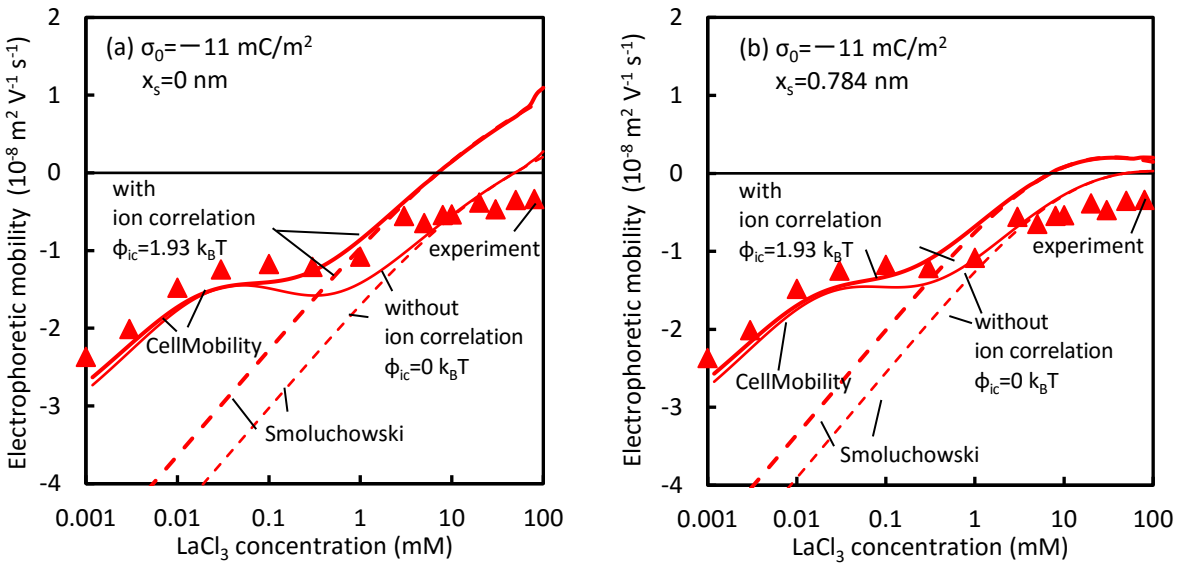

Figure 1 The relationship between electrophoretic mobility and $LaCl_3$ concentration of sulfate latex particles with the surface charge density $\sigma_0 = -11$ mC/m^2. Symbols are experimental values. Solid and dashed lines are theoretical values calculated by the CellMobility program and the Smoluchowski equation, respectively. The thin lines are calculated by without ion correlation and heavy lines are obtained with ion correlation. Calculated values in (a) assume $\psi_d = \zeta$. Calculated values in (b) assume $\psi(x_s) = \zeta$.

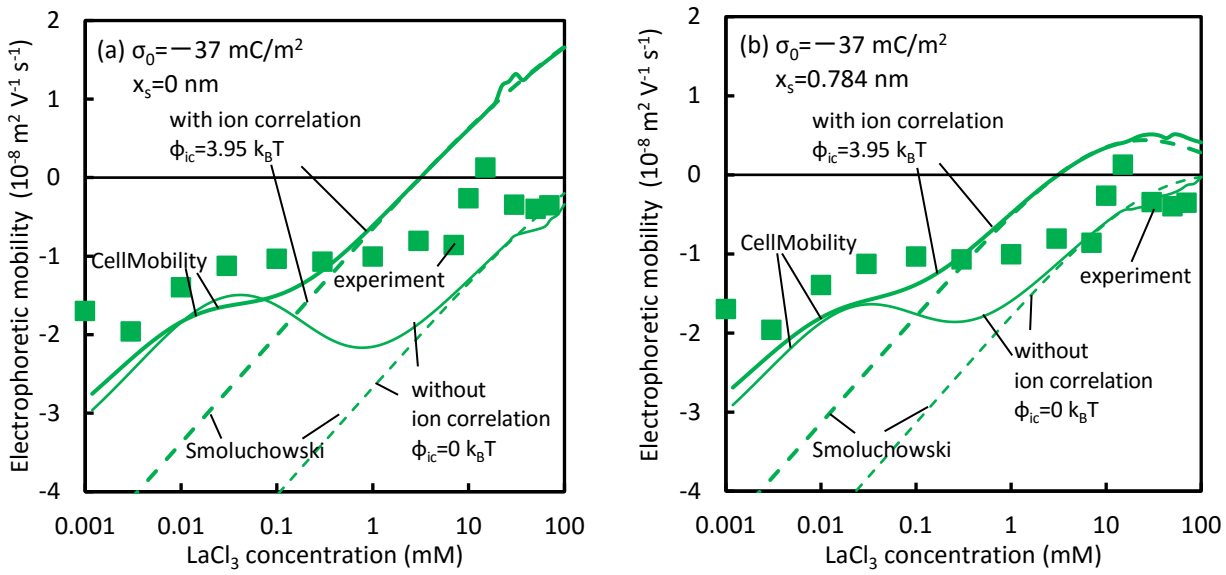

Figure 2 The relationship between electrophoretic mobility and $LaCl_3$ concentration for the sulfate latex particles with the surface charge density $\sigma_0 = -37$ mC/m^2. Symbols are experimental values. Solid and dashed lines are theoretical values calculated by the CellMobility program and the Smoluchowski equation, respectively. The thin lines are calculated by without ion correlation and heavy lines are obtained with ion correlation. Calculated values in (a) assume $\psi_d = \zeta$. Calculated values in (b) assume $\psi(x_s) = \zeta$.

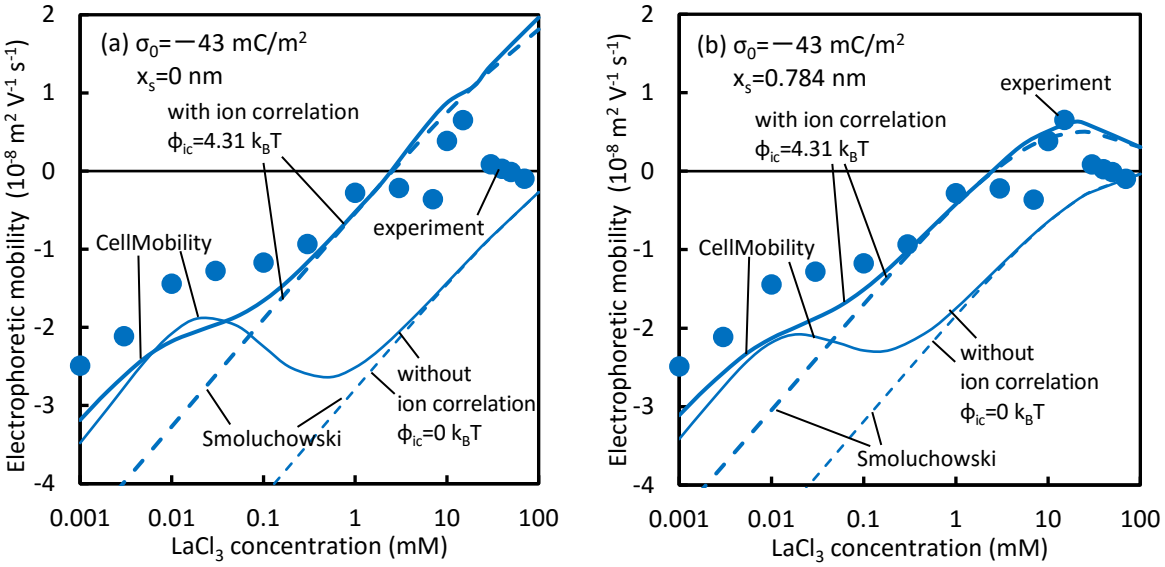

Figure 3 The relationship between electrophoretic mobility and $LaCl_3$ concentration for sulfate latex particles with the surface charge density $\sigma_0 = -43$ mC/m^2. Symbols are experimental values. The Solid and dashed lines are theoretical values calculated by the CellMobility program and the Smoluchowski equation, respectively. The thin lines are calculated by without ion correlation and heavy lines are obtained with ion correlation. Calculated values in (a) assume $\psi_d = \zeta$. Calculated values in (b) assume $\psi(x_s) = \zeta$.

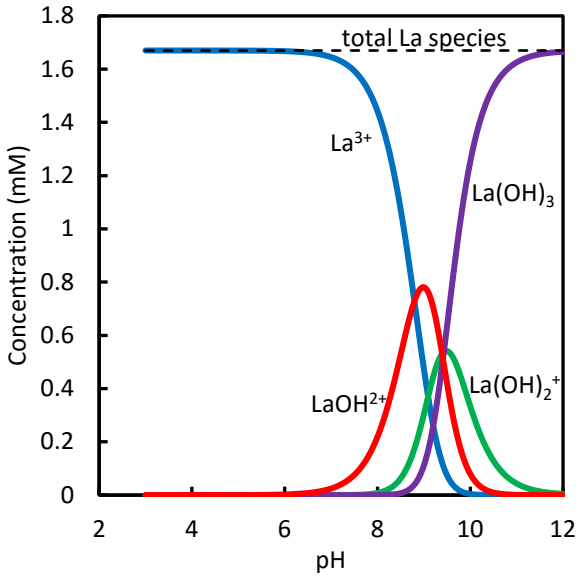

Figure 4 The concentration of hydrolyzed La species and pH in $LaCl_3$ aqueous solution with 10 mM in ionic strength. The blue line is unhydrolyzed La species. The red, green, and purple lines are hydrolyzed La species.

r

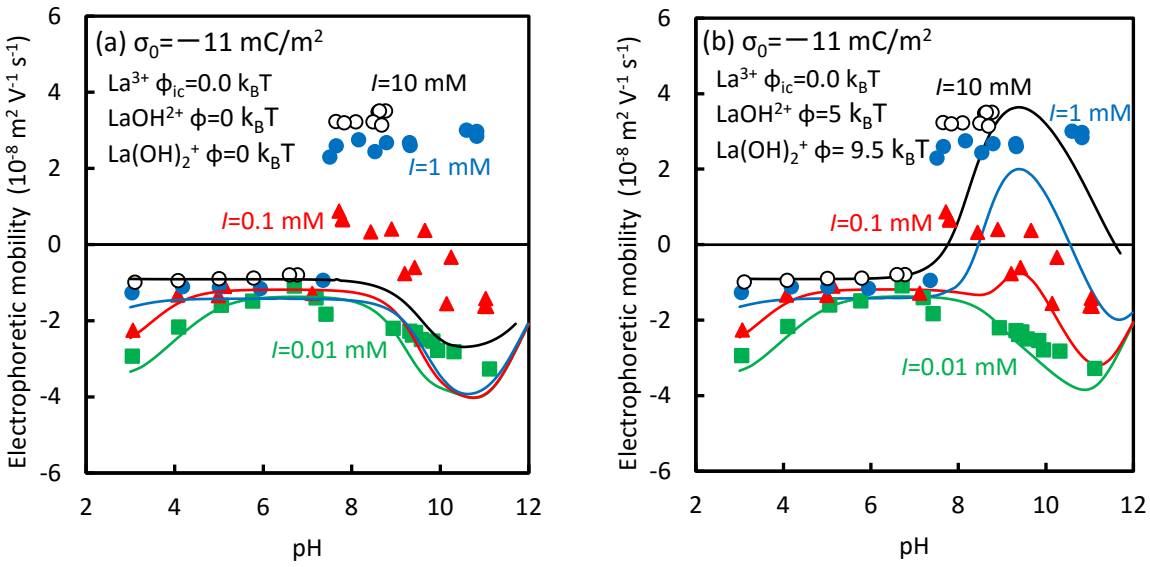

Figure 5 The relationship between electrophoretic mobility and pH in $LaCl_3$ for sulfate latex particles with the surface charge density $\sigma_0 = -11$ mC/m^2. Symbols are experimental values. Lines are theoretical values calculated by the CellMobility program. Ionic strength *I* are 0.01, 0.1, 1, and 10 from lower to upper lines. Calculated values in (a) are obtained by assuming without $LaOH^{2+}$ or $La(OH)_2^+$ adsorption and theoretical values in (b) are calculated by assuming with $LaOH^{2+}$ or $La(OH)_2^+$ adsorption

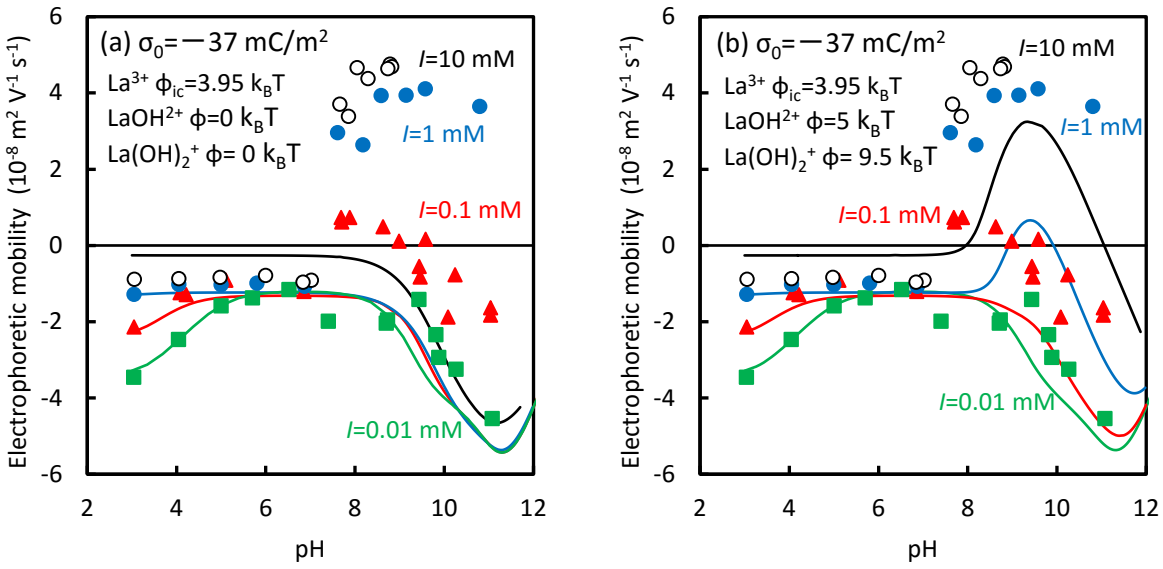

Figure 6 The relationship between electrophoretic mobility and pH in $LaCl_3$ for sulfate latex particles with the surface charge density $\sigma_0 = -37\ \mathrm{mC/m^2}$. Symbols are experimental values. Lines are theoretical values calculated by the CellMobility program. Ionic strength I are 0.01, 0.1, 1, and 10 from lower to upper lines. Calculated values in (a) are obtained by assuming without $LaOH^{2+}$ or $La(OH)_2^+$ adsorption and theoretical values in (b) are calculated by assuming with $LaOH^{2+}$ or $La(OH)_2^+$ adsorption

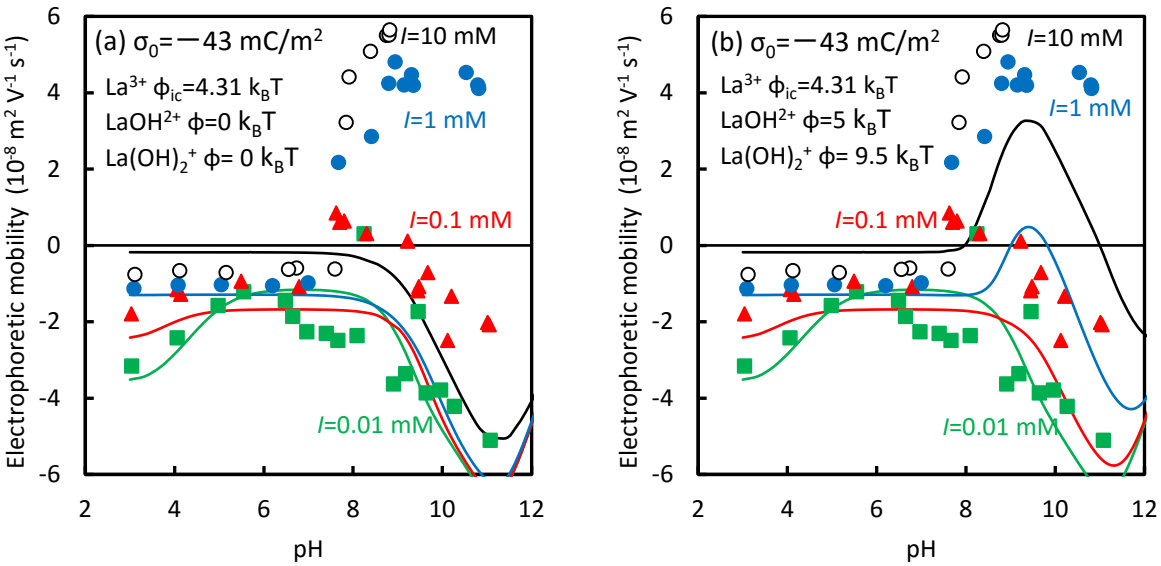

Figure 7 The relationship between electrophoretic mobility and pH in $LaCl_3$ for sulfate latex particles with the surface charge density $\sigma_0 = -43$ mC/m^2. Symbols are experimental values. Lines are theoretical values calculated by the CellMobility program. Ionic strength I are 0.01, 0.1, 1, and 10 from lower to upper lines. Calculated values in (a) are obtained by assuming without $LaOH^{2+}$ or $La(OH)_2^+$ adsorption and theoretical values in (b) are calculated by assuming with $LaOH^{2+}$ or $La(OH)_2^+$ adsorption

644
645
646
647
648 **References**
649

650 [1] W. B. Russel, D. A. Saville, and W. R. Schowalter, *Colloidal dispersions*. Cambridge
651 University Press, 1989.
652 [2] M. Elimelech, J. Gregory, and X. Jia, *Particle deposition and aggregation:*
653 *measurement, modelling and simulation*. Butterworth-Heinemann, 1998.
654 [3] V. Azari, E. Abolghasemi, A. Hosseini, S. Ayatollahi, and F. Dehghani, "Electrokinetic
655 properties of asphaltene colloidal particles: Determining the electric charge using micro
656 electrophoresis technique," *Colloids Surfaces A Physicochem. Eng. Asp.*, vol. 541, no.
657 November 2017, pp. 68–77, 2018.
658 [4] B. V. Derjaguin and L. Landau, "The theory of stability of highly charged lyophobic sols
659 and coalescence of highly charged particles in electrolyte solutions," *Acta Physicochim.*
660 *URSS*, 1941.
661 [5] E. J. W. Verwey, J. T. G. Overbeek, and J. T. G. Overbeek, "Theory of the stability of
662 lyophobic colloids," *DoverPublications. com*, 1999.
663 [6] I. Szilagyi, G. Trefalt, A. Tiraferri, P. Maroni, and M. Borkovec, "Polyelectrolyte
664 adsorption, interparticle forces, and colloidal aggregation.," *Soft Matter*, vol. 10, no. 15,
665 pp. 2479–502, Apr. 2014.
666 [7] W. F. Tan, W. Norde, and L. K. Koopal, "Humic substance charge determination by
667 titration with a flexible cationic polyelectrolyte," *Geochim. Cosmochim. Acta*, vol. 75,
668 no. 19, pp. 5749–5761, 2011.
669 [8] Y. Adachi, L. Feng, and M. Kobayashi, "Kinetics of flocculation of polystyrene latex
670 particles in the mixing flow induced with high charge density polycation near the
671 isoelectric point," *Colloids Surfaces A Physicochem. Eng. Asp.*, vol. 471, pp. 38–44,
672 2015.
673 [9] A. M. Zhivkov and R. P. Hristov, "Stability of aqueous suspensions of alumina particles
674 with adsorbed (carboxymethyl)cellulose," *Colloids Surfaces A Physicochem. Eng. Asp.*,
675 vol. 529, no. March, pp. 523–530, 2017.
676 [10] P. Somasundaran, T. W. Healy, and D. W. Fuerstenau, "Surfactant Adsorption at the
677 Solid--Liquid Interface--Dependence of Mechanism on Chain Length," *J. Phys. Chem.*,
678 vol. 68, no. 12, pp. 3562–3566, 1964.
679 [11] M. Kobayashi, S. Yuki, and Y. Adachi, "Effect of anionic surfactants on the stability

ratio and electrophoretic mobility of colloidal hematite particles," *Colloids Surfaces A Physicochem. Eng. Asp.*, vol. 510, pp. 190–197, 2016.

[12] E. L. Michor and J. C. Berg, "The particle charging behavior of ion-exchanged surfactants in apolar media," *Colloids Surfaces A Physicochem. Eng. Asp.*, vol. 512, pp. 1–6, 2017.

[13] J. Lee, "Charge carriers created by interaction of a nonionic surfactant with water in a nonpolar medium," *Colloids Surfaces A Physicochem. Eng. Asp.*, vol. 554, no. April, pp. 211–217, 2018.

[14] M. L. Jiménez, Á. V. Delgado, and J. Lyklema, "Hydrolysis versus ion correlation models in electrokinetic charge inversion: Establishing application ranges," *Langmuir*, vol. 28, no. 17, pp. 6786–6793, 2012.

[15] M. Nishiya, T. Sugimoto, and M. Kobayashi, "Electrophoretic mobility of carboxyl latex particles in the mixed solution of 1:1 and 2:1 electrolytes or 1:1 and 3:1 electrolytes: Experiments and modeling," *Colloids Surfaces A Physicochem. Eng. Asp.*, vol. 504, pp. 219–227, 2016.

[16] T. Cao, T. Sugimoto, I. Szilágyi, G. Trefalt, and M. Borkovec, "Heteroaggregation of Oppositely Charged Particles in the Presence of Multivalent Ions," *Phys. Chem. Chem. Phys.*, vol. 19, pp. 15160–15171, 2017.

[17] M. Kobayashi, "Electrophoretic mobility of latex spheres in the presence of divalent ions: Experiments and modeling," *Colloid Polym. Sci.*, vol. 286, pp. 935–940, 2008.

[18] B. Luan, K. L. Chen, and R. Zhou, "Mechanism of Divalent-Ion-Induced Charge Inversion of Bacterial Membranes," *J. Phys. Chem. Lett.*, vol. 7, no. 13, pp. 2434–2438, 2016.

[19] C. Chassagne and M. Ibanez, "Hydrodynamic size and electrophoretic mobility of latex nanospheres in monovalent and divalent electrolytes," *Colloids Surfaces A Physicochem. Eng. Asp.*, vol. 440, pp. 208–216, 2014.

[20] Y. Huang, A. Yamaguchi, T. D. Pham, and M. Kobayashi, "Charging and aggregation behavior of silica particles in the presence of lysozymes," *Colloid Polym. Sci.*, pp. 1–11, 2017.

[21] A. Hakim, M. Nishiya, and M. Kobayashi, "Charge reversal of sulfate latex induced by hydrophobic counterion: effects of surface charge density," *Colloid Polym. Sci.*, vol. 294, no. 10, pp. 1671–1678, 2016.

[22] T. Sugimoto, M. Nishiya, and M. Kobayashi, "Electrophoretic mobility of carboxyl latex particles: effects of hydrophobic monovalent counter-ions," *Colloid Polym. Sci.*, vol. 295, no. 12, pp. 2405–2411, 2017.

[23] T. Sugimoto, T. Cao, I. Szilagyi, M. Borkovec, and G. Trefalt, "Aggregation and

charging of sulfate and amidine latex particles in the presence of oxyanions," *J. Colloid Interface Sci.*, vol. 524, pp. 456–464, 2018.

[24] A. Hakim and M. Kobayashi, "Aggregation and charge reversal of humic substances in the presence of hydrophobic monovalent counter-ions: Effect of hydrophobicity of humic substances," *Colloids Surfaces A Physicochem. Eng. Asp.*, vol. 540, no. November 2017, pp. 1–10, 2018.

[25] J. Lyklema, "Overcharging, charge reversal: Chemistry or physics?," *Colloids Surfaces A Physicochem. Eng. Asp.*, vol. 291, no. 1–3, pp. 3–12, 2006.

[26] M. Quesada-Perez, A. Martin-Molina, R. Hidalgo-Alvarez, M. Quesada-Pérez, a. Martín-Molina, and R. Hidalgo-Álvarez, "Simulation of Electric Double Layers Undergoing Charge Inversion: Mixtures of Mono- and Multivalent Ions," *Langmuir*, vol. 21, no. 20, pp. 9231–9237, 2005.

[27] M. Quesada-Pérez, E. González-Tovar, A. Martín-Molina, M. Lozada-Cassou, and R. Hidalgo-Álvarez, "Ion size correlations and charge reversal in real colloids," *Colloids Surfaces A Physicochem. Eng. Asp.*, vol. 267, no. 1–3, pp. 24–30, 2005.

[28] A. Martín-Molina, M. Quesada-Pérez, and R. Hidalgo-Alvarez, "Electric double layers with electrolyte mixtures: integral equations theories and simulations.," *J. Phys. Chem. B*, vol. 110, no. 3, pp. 1326–31, 2006.

[29] A. Martín-Molina, J. A. Maroto-Centeno, R. Hidalgo-Álvarez, and M. Quesada-Pérez, "Charge reversal in real colloids: Experiments, theory and simulations," *Colloids Surfaces A Physicochem. Eng. Asp.*, vol. 319, no. 1–3, pp. 103–108, 2008.

[30] B. I. Shklovskii, "Screening of a macroion by multivalent ions: Correlation-induced inversion of charge," *Phys. Rev. E*, vol. 60, no. 5, pp. 5802–5811, 1999.

[31] F. Vereda, A. Martín Molina, R. Hidalgo-Alvarez, and M. Quesada-Pérez, "Specific ion effects on the electrokinetic properties of iron oxide nanoparticles: experiments and simulations," *Phys. Chem. Chem. Phys. Phys. Chem. Chem. Phys*, vol. 17, no. 17, pp. 17069–17078, 2015.

[32] C. Calero, J. Faraudo, and D. Bastos-González, "Interaction of monovalent ions with hydrophobic and hydrophilic colloids: Charge inversion and ionic specificity," *J. Am. Chem. Soc.*, vol. 133, no. 38, pp. 15025–15035, 2011.

[33] K. Besteman, M. A. G. Zevenbergen, and S. G. Lemay, "Charge inversion by multivalent ions: Dependence on dielectric constant and surface-charge density," *Phys. Rev. E - Stat. Nonlinear, Soft Matter Phys.*, vol. 72, pp. 1–9, 2005.

[34] C. F. Baes and R. E. Mesmer, *The hydrolysis of cations*. John Wiley & Sons Inc, 1976.

[35] L. Ramirez, S. R. Gentile, S. Zimmermann, and S. Stoll, "Comparative Study of the Effect of Aluminum Chloride , Sodium Alginate and Chitosan on the Coagulation of

752 Polystyrene Micro-Plastic Particles," *J. Colloid Sci. Biotechnol.*, vol. 5, pp. 190–198,
753 2016.
754 [36] R. T. O. James and A. D. T. W. Healy, "Adsorption of Hydrolyzable Metal Ions at the
755 Oxide-Water Interface II . Charge Reversal of SiO2 and TiO2 Colloids by Adsorbed
756 Co(ll), La(lll), and Th (IV) as Model Systems," *J. Colloid Interface Sci.*, vol. 10, no. 1,
757 pp. 53–64, 1972.
758 [37] A. Martín-Molina, C. Calero, J. Faraudo, M. Quesada-Pérez, A. Travesset, and R.
759 Hidalgo-Álvarez, "The hydrophobic effect as a driving force for charge inversion in
760 colloids," *Soft Matter*, vol. 5, no. 7, p. 1350, 2009.
761 [38] P. Sipos, P. M. May, and G. T. Hefter, "Carbonate removal from concentrated hydroxide
762 solutions," *Analyst*, vol. 125, no. 5, pp. 955–958, 2000.
763 [39] J. Kragten and L. G. Decnop-Weever, "Hydroxide Complex of Lanthanides - VIII
764 Lanthanum(III) in Perchlorate Medium," *Talanta*, vol. 34, no. 10, pp. 861–864, 1987.
765 [40] R. Kjellander, T. Åkesson, B. Jönsson, and S. Marčelja, "Double layer interactions in
766 mono- and divalent electrolytes: A comparison of the anisotropic HNC theory and
767 Monte Carlo simulations," *J. Chem. Phys.*, vol. 97, no. 2, p. 1424, 1992.
768 [41] A. Y. Grosberg, T. T. Nguyen, and B. I. Shklovskii, "Colloquium: The physics of charge
769 inversion in chemical and biological systems," *Rev. Mod. Phys.*, vol. 74, no. 2, pp. 329–
770 345, 2002.
771 [42] M. Kanduč, M. Moazzami-Gudarzi, V. Valmacco, R. Podgornik, and G. Trefalt,
772 "Interactions between charged particles with bathing multivalent counterions:
773 experiments vs. dressed ion theory," *Phys. Chem. Chem. Phys.*, vol. 19, pp. 10069–
774 10080, 2017.
775 [43] The Chemical Society of Japan, Ed., *Kagaku Binran (Ed.)*, 5th Ed. Maruzen, 2004.
776 [44] W. M. Haynes, *CRC Handbook of Chemistry and Physics, 95th Edition.* CRC Press,
777 2014.
778 [45] H. Ohshima, *Biophysical chemistry of biointerfaces*. Wiley, 2013.
779 [46] S. Ahualli, A. V. Delgado, S. J. Miklavcic, and L. R. White, "Dynamic Electrophoretic
780 Mobility of Concentrated Dispersions of Spherical Colloidal Particles. On the Consistent
781 Use of the Cell Model," *Langmuir*, vol. 22, no. 16, pp. 7041–7051, 2006.
782 [47] S. Ahualli, A. V. Delgado, S. J. Miklavcic, and L. R. White, "Use of a cell model for the
783 evaluation of the dynamic mobility of spherical silica suspensions," *J. Colloid Interface
784 Sci.*, vol. 309, no. 2, pp. 342–349, May 2007.
785 [48] B. H. Bradshaw-Hajek, S. J. Miklavcic, and L. R. White, "Dynamic Dielectric Response
786 of Concentrated Colloidal Dispersions: Comparison between Theory and Experiment,"
787 *Langmuir*, vol. 25, no. 4, pp. 1961–1969, Feb. 2009.

[49] R. W. O'Brien and L. R. White, "Electrophoretic mobility of a spherical colloidal particle," *J. Chem. Soc. Faraday Trans. 2*, vol. 74, no. 0, p. 1607, Jan. 1978.

[50] A. Martín-Molina, C. Rodríguez-Beas, R. Hidalgo-Álvarez, and M. Quesada-Pérez, "Effect of surface charge on colloidal charge reversal," *J. Phys. Chem. B*, vol. 113, pp. 6834–6839, 2009.

[51] H. Ohshima, T. W. Healy, and L. R. White, "Approximate analytic expressions for the electrophoretic mobility of spherical colloidal particles and the conductivity of their dilute suspensions," *J. Chem. Soc. Faraday Trans. 2*, vol. 79, no. 11, p. 1613, Jan. 1983.